Crystal Structure and Magnetic Properties of Hydrothermally Synthesized Barium Ferrite, $Ba_4Fe_9O_{20}H_6$*

Katsuki KITAHAMA and Ryôiti KIRIYAMA

The Institute of Scientific and Industrial Research, Osaka University, Yamadakami, Suita, Osaka 565

(Received May 4, 1976)

A new barium ferrite, $Ba_4Fe_9O_{20}H_6$, has been synthesized by a hydrothermal technique. This crystallizes in a monoclinic system with $a=10.263(5)$, $b=5.986(3)$, $c=14.559(6)$ Å, $\beta=95.20(3)°$, $Z=2$, space group C2/m. The structure was determined by Patterson and Fourier methods from three-dimensional X-ray counter data and refined by block-diagonal least-squares calculations to $R=0.098$ for 1128 reflections. The structure consists of condensed layers of ferrite anions, $Fe(OH)_6^{3-}$ clusters, and Ba^{2+} cations; it has the character of a crystal growth from aqueous solutions. The presence of Fe^{2+} was confirmed; such ions are located in the condensed ferrite layer. Consequently, the true formula should be written as $Ba_4[Fe^{III}(OH)_6][Fe^{II}Fe_7^{III}O_{14}]$. This crystal is ferrimagnetic below the Nèel point of 515 K. The magnetic moment was estimated to be about 10 μ_B per formula unit at 0 K.

The BaO–Fe_2O_3 and BaO–Fe_2O_3–MeO systems have been studied by many workers because of their great importance as useful magnetic materials. Most of them have been synthesized by firing or flux methods at temperatures higher than 700 °C.[1,2] Hydrothermal syntheses of these substances seem worthwhile, not only for the manufacture of magnetic materials but for the reaction chemistry with respect to the amphoteric behavior of Fe^{3+} ions in aqueous solutions. Of these, barium monoferrite, $BaFe_2O_4$, has an interesting structure characterized by wide-open cavities.[3] In the early stage of hydrothermal studies, our aim was to ascertain whether Ba^{2+} cations leach through the channels of this structure, as is often observed in zeolites, or not. Such hydrothermal treatments and growth of new barium ferrites, however, revealed that the reaction proceeds through dissolution of the starting material. By processing $Ba(OH)_2$ and Fe_2O_3 under hydrothermal conditions, four kinds of barium ferrite were obtained: these are $Ba_4Fe_9O_{20}H_6$, $Ba_8Fe_{13}O_{30}H_6$,[4] and two modifications of $BaFe_4O_7$.[5,6] Successive X-ray studies showed that their crystal structures certainly reflect some characteristics of the crystal growth from aqueous solutions. This paper is concerned with the crystal structure and magnetic properties of $Ba_4Fe_9O_{20}H_6$. This substance was designated Phase II among the hydrothermal products and was considered to have the structure of a modified Y ferrite in a previous paper.[7]

Experimental

Preparation. Barium hydroxide octahydrate (0.63 g), and α-Fe_2O_3 (0.32 g), both of which were commercial guaranteed reagent grade, and 5 ml of distilled water were charged in a platinum capsule with a lid. The capsule was inserted into a Morey bomb sealed with a copper gasket. The contents were heated at a rate of 4 °C min^{-1} up to 300 °C, kept at this temperature for 5 days, and then quenched into ice water. The pressure inside the bomb during the reaction was roughly estimated as 150 bar from a filling ratio-temperature diagram given by Kennedy.[8] Partial reduction of Fe^{3+} to Fe^{2+} may be caused by hydrogen, probably resulting from corrosion of the stainless steel vessel by water. In fact, for a shorter reaction period of one or two days, where the reduction was not enough, the product was contaminated with a hexagonal phase ($P6_3/m$) of $BaFe_4O_7$. The crystalline product was filtered and then washed with distilled water. The obtained crystals were platy hexagons in shape and were strongly magnetic, so they could be easily separated by use of a hand magnet.

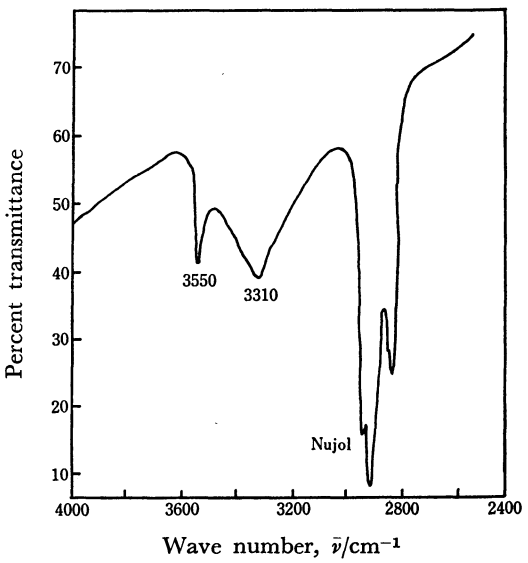

Fig. 1. Infrared spectra of $Ba_4Fe_9O_{20}H_6$.

Chemical Composition. The molar ratio of Ba/Fe was determined as 4 : 8.89 from an ordinary gravimetry measurement and as 4 : 8.80 by a fluorescent X-ray analysis; these values agree within their experimental errors. The presence of OH groups was evidenced by IR spectroscopy. As shown in Fig. 1, the two OH stretching bands occurred at about 3550 and 3310 cm^{-1}, whereas no peak were observed in the region 1500—1800 cm^{-1}. The weight loss corresponding to $3H_2O$ was found at about 695 K by means of TG analysis; from this the amount of H could be determined. The presence of ferrous ions was detected from the color test of $K_3Fe(CN)_6$ in an aqueous solution. Although its amount was roughly estimated from iodometry, the exact content was successfully determined by referring to the number of peaks assigned to oxygen atoms in the electron density maps described below.

X-Ray Data Collections. The crystals synthesized hydrothermally were dark red transparent hexagonal plates; almost all crystals were twins or aggregates grown epitaxially. A

* Thesis submitted by one of the authors(K.K.) to Osaka University in partial fulfillment of the requirements for the degree of Doctor of Science.

Table 1. Crystal data for $Ba_4Fe_9O_{20}H_6$

Space group C2/m	$\rho_{obsd}=5.06$ g cm^{-3}
$a=10.263(5)$ Å	$\rho_{calcd}=5.137$
$b=5.986(3)$	$F(000)=1248$ e cell^{-1}
$c=14.559(6)$	F. W. $=1377.98$ g mol^{-1}
$\beta=95.20(3)°$	$V=890.72$ Å^3
$Z=2$	$\mu_{MoK\alpha}=158.9$ cm^{-1}

single crystal happened to be found with the shape of an irregular hexagonal plate with dimensions of $0.08\times0.04\times0.015$ mm^3; this crystal was used for the present X-ray study. Weissenberg and precession photographs indicated the crystal to be monoclinic, with a space group either C2, Cm, or C2/m; the last group was confirmed by solution of the structure (the systematic absences: hkl, $h+k$ odd). The same crystal was mounted on a Rigaku four-circle diffractometer with its c-axis along the ϕ-axis of the goniostat. The lattice parameters were determined from the setting angles of the same diffractometer, using Mo$K\alpha_1$ radiation. The results are listed in Table 1 together with other crystal data. Intensity data were collected by use of zirconium-filtered Mo$K\alpha$ radiation, with a 2θ-ω scan mode. The scan speed was 1°min^{-1} in 2θ and background intensities were measured for 10 s at both ends of the scan. In total, 1128 independent reflections with $\sin\theta/\lambda$ less than 0.65 Å^{-1} were measured. The reference reflections that were monitored periodically showed no significant intensity fluctuations during the collection of intensity data. For reflections having scan counts below the background levels, the intensity values were taken as 0.0. No corrections were made for absorption or extinction.

Magnetization. Magnetic properties were measured by means of a Faraday method on a Naruse electro-mechanical balance equipped with an automated recording device. The values of magnetization were calibrated by using powdered nickel (99.999%).

Mössbauer Spectroscopy. The measurement was made on a Hitachi AA40 Mössbauer spectrometer with a ^{57}Co(Pd) source moving against a specimen in a constant acceleration mode. An iron foil was used for the calibration of velocity.

Structure Determination and Refinement

Three-dimensional Patterson maps showed peaks only on the planes at $y=0$, 1/2, and at about $y=1/4$, and suggested the presence of mirror planes perpendicular to the b-axis. Because these peaks were comparable in height, owing to the periodical stacking of oxygens, Patterson maps were calculated again with reflections of $\sin\theta/\lambda>0.4$ Å^{-1} and with a sharpening factor of $B=2.0$ Å^2. (Of the 1128 reflections, 280 were eliminated from this calculation; the sum of $|F_o|$ of these 280 reflections amounts to 50% of the $\Sigma|F_o|$ of the total reflections.) Such a modification of the Patterson function resolved the diffuse peaks and was helpful in solving the structure. Thus the positions of Ba and Fe were easily determined. All positions of oxygen atoms were found on successive three-dimensional electron density maps phased with Ba and Fe atoms. Although a full-matrix least-squares refinement was started from these atomic positions in the isotropic mode, the structure did not converge below $R=0.15$. Therefore, the block-diagonal least-squares refinement was performed, varing the individual isotropic thermal parameters, an overall temperature factor, and a scale factor. At the stage of $R=0.118$, anisotropic thermal parameters were introduced for Ba an Fe atoms. Difference Fourier maps computed at this stage showed no ripple higher than 2.0 e Å^{-1}. After four further cycles of refinement, R dropped to 0.098. No atomic parameters shifted by more than one fourth of their associated standard deviations in the final cycle. The scattering factors for Ba^{2+}, Fe^{3+} (applied for all Fe), and O^- were taken from *International Tables for X-Ray Crystallography, Vol. IV.*[9] The quantity minimized during the least-squares procedure was $\Sigma w(|F_o|-|F_c|)^2$, all weights being unity. All computations were performed on the NEAC 2200/700 computer of this university, using local modifications of RSSFR-5, RSFLS, HBLS V, and RSDA-4 in the UNICS program system,[10] and the stereoscopic drawing program ORTEP written by Johnson.[11] The observed and calculated structure factors are compared in Table 2. The final positional thermal parameters are given in Table 3.

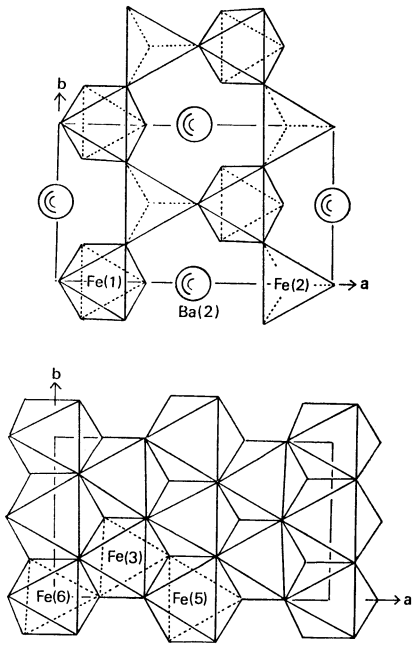

Fig. 2. Two kinds of slices in the condensed ferrite layer viewed along the c* direction. Above: one of the outer slices of the triple layer ($z\approx0.19$). Below: a middle sheet of the triple layer.

Results and Discussion

Crystal Structure. The structure consists of eminent triple layers of oxygen coordination polyhedra around Fe atoms parallel to the (001) plane, and Fe-$(OH)_6^{3-}$ anion clusters and Ba^{2+} cations both intervening between triple layers. Of the nine Fe atoms in the chemical formula, seven atoms are coordinated octahedrally by oxygen atoms while the other two are surrounded tetrahedrally. The triple layer is composed of two kinds of slices: that is, one type is sandwiched between the others. As shown in Fig. 2, each

Table 2. Observed and calculated structure factors ($\times 1/2$) for $Ba_4Fe_9O_{20}H_6$

H	FO	FC
K = 0 L = 0		
2	30	29
4	10	15
6	115	117
8	105	97
10	42	46
12	0	4
K = 0 L = 1		
-12	82	83
-10	56	56
-8	63	60
-6	47	51
-4	164	180
-2	44	47
0	45	43
2	69	72
4	68	70
6	108	114
8	74	71
10	11	9
12	22	21
K = 0 L = 2		
-12	157	154
-10	0	4
-8	28	26
-6	76	79
-4	38	32
-2	83	94
0	19	19
2	21	30
4	88	90
6	112	111
8	129	140
10	20	16
12	11	8
K = 0 L = 3		
-12	32	32
-10	16	19
-8	30	23
-6	186	183
-4	53	43
-2	34	46
0	56	60
2	100	106
4	107	129
6	51	61
8	58	60
10	0	0
12	132	129
K = 0 L = 4		
-12	9	7
-10	0	12
-8	29	24
-6	52	43
-4	213	245
-2	0	17
0	121	142
2	130	151
4	123	138
6	61	66
8	129	134
10	28	25
12	23	18
K = 0 L = 5		
-12	25	21
-10	34	25
-8	144	137
-6	69	70
-4	74	83
-2	0	6
0	236	272
2	18	14
4	53	57
6	61	66
8	11	8
10	91	94
12	14	17
K = 0 L = 6		
-12	117	100
-10	108	92
-8	31	22
-6	49	54
-4	182	206
-2	0	7
0	87	82
2	33	32
4	82	91
6	81	85
8	24	21
10	32	36
12	13	5
K = 0 L = 7		
-12	78	58
-10	48	47
-8	9	12
-6	32	29
-4	64	64
-2	131	139
0	6	5
2	42	39
4	17	19
6	82	77
8	95	96
10	16	16
K = 0 L = 8		
-12	40	32
-10	0	9
-8	54	52
-6	121	119
-4	37	44
-2	120	125
0	15	8
2	43	37
4	247	253
6	67	68
8	32	33
10	32	33
K = 0 L = 9		
-12	10	8
-10	57	48
-8	59	53
-6	5	0
-4	105	104
-2	0	3
0	91	90
2	114	110
4	38	40
6	11	11
8	68	65
10	25	27
K = 0 L = 10		
-10	13	13
-8	178	170
-6	60	59
-4	37	37
-2	44	45
0	139	140
2	21	13
4	19	14
6	48	52
8	17	14
10	67	71
K = 0 L = 11		
-10	58	54
-8	33	29
-6	13	10
-4	71	71
-2	97	93
0	34	35
2	26	27
4	18	21
6	96	90
8	0	8
10	45	41
K = 0 L = 12		
-10	31	33
-8	17	10
-6	29	26
-4	44	38
-2	71	71
0	126	117
2	21	17
4	55	50
6	14	21
8	66	65
K = 0 L = 13		
-10	0	1
-8	18	12
-6	93	85
-4	33	29
-2	96	89
0	31	18
2	44	41
4	143	136
6	21	19
8	0	7
K = 0 L = 14		
-8	73	67
-6	71	65
-4	53	50
-2	23	23
0	107	103
2	77	77
4	12	8
6	14	12
8	75	81
K = 0 L = 15		
-8	84	75
-6	10	13
-4	0	8
-2	12	16
0	18	31
2	65	55
4	28	30
6	12	6
K = 0 L = 16		
-8	37	32
-6	0	10
-4	98	92
-2	85	77
0	3	3
2	47	38
4	18	9
6	30	39
K = 0 L = 18		
-4	74	67
-2	68	69
0	15	33
2	0	5
-4	74	67
-2	68	69
0	15	13
2	0	5
K = 1 L = 0		
1	9	14
3	224	232
5	39	36
7	47	47
9	30	29
11	25	24
13	46	47
K = 1 L = 1		
-13	28	33
-11	7	11
-9	39	40
-7	57	60
-5	37	34
-3	16	14
-1	18	7
1	45	42
3	114	113
5	88	83
7	8	9
9	105	106
11	86	77
13	0	9
K = 1 L = 2		
-13	16	14
-11	13	13
-9	109	105
-7	8	18
-5	64	58
-3	5	8
-1	5	3
1	114	98
3	118	117
5	38	47
7	32	32
9	81	74
11	52	58
K = 1 L = 3		
-13	0	1
-11	3	8
-9	123	122
-7	74	68
-5	20	26
-3	188	195
-1	140	122
1	59	61
3	44	42
5	58	62
7	22	30
9	88	90
11	0	4
K = 1 L = 4		
-13	35	32
-11	48	43
-9	42	34
-7	30	28
-5	24	20
-3	15	2
-1	143	141
1	30	33
3	57	68
5	111	126
7	41	44
9	30	26
11	20	13
K = 1 L = 5		
-13	33	25
-11	48	45
-9	0	0
-7	25	25
-5	41	48
-3	126	140
-1	32	28
1	39	31
3	136	149
5	41	46
7	97	107
9	0	9
11	28	29
K = 1 L = 6		
-11	13	9
-9	63	64
-7	104	103
-5	17	22
-3	19	22
-1	55	54
1	3	4
3	94	95
5	54	56
7	36	37
9	75	78
11	53	57
K = 1 L = 7		
-11	24	22
-9	45	43
-7	72	74
-5	96	100
-3	20	17
-1	103	95
1	121	105
3	71	69
5	16	13
7	26	26
9	39	38
11	45	49
K = 1 L = 8		
-11	21	25
-9	81	84
-7	27	23
-5	54	55
-3	116	114
-1	43	36
1	162	150
3	6	1
5	9	12
7	94	96
9	83	85
11	0	0
K = 1 L = 9		
-11	28	25
-9	10	15
-7	16	15
-5	8	6
-3	12	16
-1	89	82
1	16	8
3	19	19
5	87	90
7	31	31
9	27	26
K = 1 L = 10		
-11	82	76
-9	0	1
-7	17	19
-5	92	92
-3	80	78
-1	12	1
1	5	6
3	88	86
5	40	40
7	86	87
9	26	27
K = 1 L = 11		
-11	20	28
-9	20	20
-7	55	55
-5	90	88
-3	45	43
-1	26	24
1	102	90
3	112	111
5	39	38
7	15	8
9	66	67
K = 1 L = 12		
-9	13	12
-7	49	50
-5	49	48
-3	23	17
-1	69	64
1	38	34
3	39	32
5	14	6
7	15	13
9	26	24
K = 1 L = 13		
-9	64	66
-7	18	16
-5	26	19
-3	77	74
-1	25	27
1	128	110
3	25	19
5	29	28
7	76	75
K = 1 L = 14		
-9	43	34
-7	12	12
-5	45	38
-3	73	68
-1	51	49
1	13	3
3	30	28
5	61	69
7	44	41
K = 1 L = 15		
-7	0	5
-5	53	51
-3	20	13
-1	49	38
1	31	23
3	0	5
5	54	56
K = 1 L = 16		
-7	38	35
-5	80	72
-3	27	27
-1	46	48
1	66	65
3	50	56
5	38	26
K = 1 L = 17		
-5	29	38
-3	13	2
-1	46	54
1	19	19
3	48	42
K = 1 L = 18		
-3	10	11
-1	16	19
1	65	85
K = 2 L = 0		
0	266	262
2	140	123
4	23	18
6	209	216
8	31	24
10	30	34
12	36	32
K = 2 L = 1		
-12	27	31
-10	108	108
-8	0	2
-6	136	137
-4	52	50
-2	146	131
0	52	44
2	13	4
4	24	18
6	63	62
8	99	93
10	0	10
12	54	53
K = 2 L = 2		
-12	98	92
-10	32	21
-8	13	9
-6	173	172
-4	12	7
-2	145	126
0	98	80
2	125	112
4	62	55
6	65	59
8	39	49
10	48	46
12	14	16
K = 2 L = 3		
-12	62	59
-10	22	19
-8	10	1
-6	145	144
-4	109	100
-2	93	100
0	151	122
2	19	4
4	26	33
6	129	140
8	11	11
10	45	43
12	83	84
K = 2 L = 4		
-12	32	34
-10	19	21
-8	41	38
-6	43	48
-4	79	85
-2	49	56
0	39	26
2	327	323
4	51	56
6	85	92
8	51	52
10	65	67
12	13	11
K = 2 L = 5		
-12	54	50
-10	37	39
-8	61	63
-6	118	126
-4	20	22
-2	97	111
0	207	177
2	49	43
4	98	99
6	89	97
8	22	27
10	64	67
12	31	35
K = 2 L = 6		
-12	59	53
-10	158	148
-8	7	1
-6	76	85
-4	73	88
-2	28	30
0	58	41
2	49	49
4	13	15
6	77	79
8	58	62
10	87	95
K = 2 L = 7		
-12	54	45
-10	0	15
-8	53	54
-6	41	45
-4	81	90
-2	61	59
0	77	64
2	26	22
4	61	57
6	0	7
8	33	35
10	63	63
K = 2 L = 8		
-12	47	45
-10	32	38
-8	0	9
-6	83	90
-4	51	54
-2	206	230
0	62	48
2	46	43
4	118	120
6	102	107
8	8	10
10	83	81
K = 2 L = 9		
-10	18	11
-8	12	20
-6	54	66
-4	38	45
-2	84	83
0	18	9
2	156	147
4	0	3
6	26	24
8	34	37
10	0	2
K = 2 L = 10		
-10	58	58
-8	95	103
-6	68	74
-4	0	6
-2	114	119
0	124	108
2	21	15
4	72	72
6	93	95
8	21	24
10	29	36
K = 2 L = 11		
-10	62	60
-8	56	58
-6	30	32
-4	47	49
-2	58	56
0	104	94
2	24	22
4	24	27
6	30	33
8	52	52
K = 2 L = 12		
-10	21	14
-8	38	40
-6	61	64
-4	60	64
-2	17	11
0	35	25
2	14	15
4	0	4
6	95	90
8	38	36
K = 2 L = 13		
-8	24	24
-6	0	15
-4	13	25
-2	121	123
0	46	39
2	12	9
4	107	103
6	48	46
8	26	31
K = 2 L = 14		
-8	25	23
-6	104	110
-4	34	33
-2	46	47
0	47	44
2	93	92
4	17	15
6	32	30
K = 2 L = 15		
-8	65	66
-6	14	16
-4	33	28
-2	25	33
0	0	0
2	16	5
4	64	65
6	41	39
K = 2 L = 16		
-6	37	36
-4	51	52
-2	45	49
0	51	55
2	99	93
4	6	15
K = 2 L = 17		
-4	46	52
-2	8	1
0	31	29
2	9	8
K = 2 L = 18		
-2	61	77
0	9	5
K = 3 L = 0		
1	11	15
3	200	195
5	35	24
7	41	41
9	30	23
11	28	25
K = 3 L = 1		
-11	8	5
-9	39	39
-7	55	53
-5	30	24
-3	0	10
-1	9	9
1	38	33
3	106	99
5	92	83
7	9	7
9	92	93
11	72	70
K = 3 L = 2		
-11	19	13
-9	98	94
-7	16	22
-5	54	51
-3	12	5
-1	0	0
1	97	83
3	125	106
5	38	38
7	36	31
9	68	64
11	51	53
K = 3 L = 3		
-11	6	6
-9	114	113
-7	73	65
-5	15	17
-3	163	155
-1	111	97
1	50	51
3	53	44
5	56	51
7	27	32
9	80	85
11	0	3
K = 3 L = 4		
-11	41	39
-9	44	37
-7	21	25
-5	25	19
-3	0	5
-1	121	117
1	27	26
3	61	57
5	108	108
7	44	44
9	24	23
11	20	13
K = 3 L = 5		
-11	49	43
-9	8	4
-7	25	23
-5	47	50
-3	119	126
-1	25	21
1	47	39
3	137	126
5	35	38
7	88	91
9	0	6
11	22	31
K = 3 L = 6		
-11	7	11
-9	55	58
-7	92	92
-5	0	14
-3	0	15
-1	39	40
1	15	8
3	95	86
5	51	48
7	31	31
9	66	72
11	53	55
K = 3 L = 7		
-11	21	23
-9	40	36
-7	62	66
-5	79	86
-3	15	11
-1	94	92
1	114	94
3	63	60
5	0	3
7	26	23
9	38	38
K = 3 L = 8		
-11	11	24
-9	76	80
-7	23	17
-5	43	45
-3	97	100
-1	37	36
1	149	131
3	12	2
5	7	9
7	86	88
9	72	75
K = 3 L = 9		
-11	20	23
-9	20	15
-7	0	8
-5	0	2
-3	0	12
-1	68	70
1	8	8
3	24	24
5	80	82
7	32	30
9	25	27
K = 3 L = 10		
-9	4	4
-7	19	19
-5	77	83
-3	62	66
-1	0	0
1	0	4
3	81	77
5	41	36
7	80	83
9	27	24
K = 3 L = 11		
-9	26	21
-7	57	53
-5	76	83
-3	39	42
-1	15	16
1	87	74
3	104	99
5	37	35
7	15	2
K = 3 L = 12		
-9	0	10
-7	46	45
-5	43	50
-3	0	15
-1	55	58
1	32	28
3	32	29
5	12	3
7	10	13
K = 3 L = 13		
-9	59	61
-7	7	14
-5	15	14
-3	65	70
-1	22	20
1	111	103
3	0	15
5	28	29
7	69	69
K = 3 L = 14		
-7	8	14
-5	27	34
-3	60	63
-1	44	47
1	11	3
3	16	23
5	63	63
K = 3 L = 15		
-7	8	6
-5	42	44
-3	18	10
-1	37	34
1	20	19
3	11	9
5	51	53
K = 3 L = 16		
-5	70	69
-3	20	22
-1	39	42
1	68	61
3	46	54
K = 3 L = 17		
-3	13	0
-1	35	48
1	0	20
K = 4 L = 0		
0	339	344
2	31	19
4	20	21
6	95	91
8	78	74
10	36	43
K = 4 L = 1		
-10	48	48
-8	55	51
-6	38	41
-4	129	121
-2	35	31
0	42	25
2	56	51
4	64	55
6	96	96
8	59	57
10	8	11
K = 4 L = 2		
-10	0	5
-8	21	22
-6	62	58
-4	27	24
-2	81	77
0	0	4
2	15	13
4	56	50
6	102	90
8	104	107
10	12	11
K = 4 L = 3		
-10	19	18
-8	16	19
-6	152	147
-4	45	32
-2	20	29
0	61	43
2	92	74
4	96	97
6	47	49
8	51	46
10	15	1
K = 4 L = 4		
-10	16	13
-8	19	18
-6	35	32
-4	163	161
-2	14	9
0	110	99
2	130	116
4	112	102
6	48	50
8	106	106
10	25	19
K = 4 L = 5		
-10	25	19
-8	112	111
-6	53	56
-4	56	55
-2	10	11
0	228	195
2	22	18
4	44	38
6	51	50
8	14	4
10	72	82
K = 4 L = 6		
-10	84	77
-8	24	21
-6	37	41
-4	135	144
-2	10	6
0	54	39
2	29	26
4	65	62
6	74	77
8	21	19
10	29	30
K = 4 L = 7		
-10	39	41
-8	0	11
-6	14	17
-4	43	49
-2	96	106
0	8	2
2	44	36
4	8	8
6	63	60
8	77	79
K = 4 L = 8		
-10	14	10
-8	41	39
-6	93	100
-4	22	28
-2	84	93
0	8	5
2	37	26
4	193	192
6	50	54
8	32	30
K = 4 L = 9		
-10	45	41
-8	41	42
-6	0	1
-4	72	83
-2	12	4
0	82	72
2	95	87
4	32	32
6	0	8
8	56	56
K = 4 L = 10		
-8	130	140
-6	42	46
-4	31	33
-2	29	36
0	123	111
2	22	18
4	19	14
6	41	40
8	23	12
K = 4 L = 11		
-8	22	23
-6	11	8
-4	54	59
-2	71	80
0	31	31
2	26	23
4	13	13
6	69	77
K = 4 L = 12		
-8	22	5
-6	19	18
-4	27	32
-2	52	57
0	100	87
2	21	17
4	45	41
6	17	19
K = 4 L = 13		
-6	65	71
-4	28	25
-2	65	72
0	0	13
2	35	32
4	122	117
K = 4 L = 14		
-6	51	54
-4	44	43
-2	23	19
0	89	85
2	64	61
4	0	5
K = 4 L = 15		
-4	17	8
-2	6	11
0	24	26
2	51	47
K = 4 L = 16		
-2	58	69
0	0	1
K = 5 L = 0		
1	11	11
3	153	149
5	36	27
7	28	36
9	20	20
K = 5 L = 1		
-9	31	34
-7	49	51
-5	36	29
-3	16	9
-1	5	8
1	31	24
3	76	76
5	65	58
7	11	0
9	81	86
K = 5 L = 2		
-9	85	79
-7	0	14
-5	46	45
-3	0	0
-1	8	11
1	79	72
3	88	80
5	25	28
7	26	26
9	64	59
K = 5 L = 3		
-9	93	95
-7	55	48
-5	11	14
-3	142	138
-1	93	79
1	38	39
3	21	17
5	45	40
7	20	22
9	67	70
K = 5 L = 4		
-9	29	25
-7	3	16
-5	21	16
-3	13	3
-1	95	95
1	31	27
3	45	47
5	96	90
7	34	30
9	29	22
K = 5 L = 5		
-9	3	4
-7	17	14
-5	30	39
-3	92	95
-1	15	18
1	18	13
3	105	100
5	34	35
7	81	85
9	12	5
K = 5 L = 6		
-9	54	52
-7	80	75
-5	19	19
-3	12	9
-1	33	31
1	14	7
3	77	72
5	51	48
7	19	22
K = 5 L = 7		
-9	37	34
-7	52	61
-5	66	77
-3	18	18
-1	60	63
1	83	76
3	57	49
5	8	12
7	15	19
K = 5 L = 8		
-9	68	67
-7	22	24
-5	36	37
-3	74	83
-1	24	23
1	110	104
3	0	0
5	17	7
7	69	73
K = 5 L = 9		
-7	17	14
-5	0	4
-3	15	19
-1	61	65
1	12	2
3	0	12
5	65	66
7	15	23
K = 5 L = 10		
-7	11	15
-5	57	71
-3	52	60
-1	9	2
1	13	9
3	63	60
5	33	34
K = 5 L = 11		
-7	35	39
-5	60	66
-3	25	32
-1	16	17
1	74	73
3	83	86
5	28	31
K = 5 L = 12		
-5	25	36
-3	14	9
-1	43	50
1	27	29
3	29	23
K = 5 L = 13		
-5	21	17
-3	44	55
-1	21	20
1	89	84
3	0	14
K = 5 L = 14		
-3	45	52
-1	32	36
1	0	2
K = 6 L = 0		
0	155	156
2	77	66
4	18	12
6	135	131
8	21	13
K = 6 L = 1		
-8	14	5
-6	84	86
-4	33	34
-2	76	74
0	26	31
2	0	1
4	8	4
6	39	47
8	65	70
K = 6 L = 2		
-8	6	10
-6	103	99
-4	15	16
-2	57	56
0	54	54
2	57	52
4	53	51
6	48	41
8	29	33
K = 6 L = 3		
-8	0	7
-6	90	95
-4	70	67
-2	55	59
0	82	78
2	18	6
4	22	26
6	93	90
8	0	6
K = 6 L = 4		
-8	33	32
-6	23	25
-4	48	53
-2	36	40
0	24	21
2	182	172
4	37	35
6	68	67
K = 6 L = 5		
-8	38	47
-6	76	87
-4	0	10
-2	62	68
0	115	106
2	29	22
4	62	63
6	65	68
K = 6 L = 6		
-6	60	52
-4	53	53
-2	17	18
0	40	39
2	17	23
4	8	0
6	48	54
K = 6 L = 7		
-6	32	31
-4	58	68
-2	38	42
0	45	44
2	0	8
4	40	41
6	9	5
K = 6 L = 8		
-6	58	62
-4	32	35
-2	118	134
0	38	37
2	28	28
4	83	86
K = 6 L = 9		
-6	39	45
-4	28	30
-2	63	53
0	12	13
2	109	102
4	13	4
K = 6 L = 10		
-4	6	3
-2	67	76
0	69	65
2	4	6
4	54	54
K = 6 L = 11		
-4	16	28
-2	36	42
0	61	67
2	0	14
K = 6 L = 12		
0	20	14
K = 7 L = 0		
1	10	14
3	115	116
5	16	12
K = 7 L = 1		
-5	23	16
-3	0	7
-1	17	9
1	17	17
3	58	63
5	55	58
K = 7 L = 2		
-5	31	36
-3	9	2
-1	0	9
1	60	60
3	68	71
5	18	18
K = 7 L = 3		
-5	10	3
-3	87	96
-1	63	58
1	19	29
3	23	25
5	32	29
K = 7 L = 4		
-5	4	14
-3	5	6
-1	62	71
1	17	18
3	34	37
K = 7 L = 5		
-3	74	82
-1	15	11
1	21	22
3	79	76
K = 7 L = 6		
-3	15	5
-1	21	17
1	6	12
3	53	61
K = 7 L = 7		
-3	0	11
-1	50	63
1	61	63
K = 7 L = 8		
-1	20	24

of the FeO_6 octahedra forming the middle slice shares its edges with six adjacent octahedra within the same slice. In both outer slices, each FeO_6 octahedron shares its vertices with three FeO_4 tetrahedra within the same slice and *vice versa* to form the six-membered ring of oxygen atoms around a Ba(2). Of the six independent Fe, only Fe(2) is coordinated tetrahedrally. Fe(3), Fe(5), and Fe(6) belong to the middle slice of the triple layer, while Fe(1) and Fe(2) belong to its outer slices. Fe(4) is situated at the center of the

TABLE 3. FINAL POSITIONAL PARAMETERS ($\times 10^4$) AND THERMAL PARAMETERS ($Å^2 \times 10^2$)[a]

	x/a	y/b	z/c	B_{11} or B	B_{22}	B_{33}	B_{12}	B_{13}	B_{23}
Ba(1)	1445(2)	0	4138(2)	86(6)	59(6)	69(6)	0	−17(5)	0
Ba(2)	5295(2)	0	2189(2)	68(6)	12(6)	210(8)	0	−1(5)	0
Fe(1)	1926(4)	0	1755(4)	55(14)	22(13)	36(13)	0	−7(11)	0
Fe(2)	8595(4)	0	2068(4)	50(13)	18(13)	53(14)	0	−15(11)	0
Fe(3)	2500	2500	0	59(13)	15(13)	53(13)	−10(11)	−2(10)	9(11)
Fe(4)	5000	0	5000	63(20)	50(20)	30(19)	0	−1(15)	0
Fe(5)	5000	0	0	180(28)	109(26)	205(29)	0	−4(23)	0
Fe(6)	0	0	0	21(18)	31(19)	36(19)	0	−3(14)	0
O(1)	970(13)	2341(15)	761(13)	74(21)					
O(2)	2805(14)	2401(16)	2461(14)	108(24)					
O(3)	3906(15)	2429(17)	4346(14)	119(24)					
O(4)	3338(19)	0	765(19)	64(30)					
O(5)	386(18)	0	2438(18)	36(28)					
O(6)	3808(22)	0	6019(22)	117(36)					
O(7)	8447(20)	0	743(20)	70(31)					

a) Estimated standard deviations are given in parentheses. The anisotropic thermal factors are of the form $T=\exp\left[-\frac{1}{4}(h^2a^{*2}B_{11}+\cdots+2klb^*c^*B_{23})\right]$.

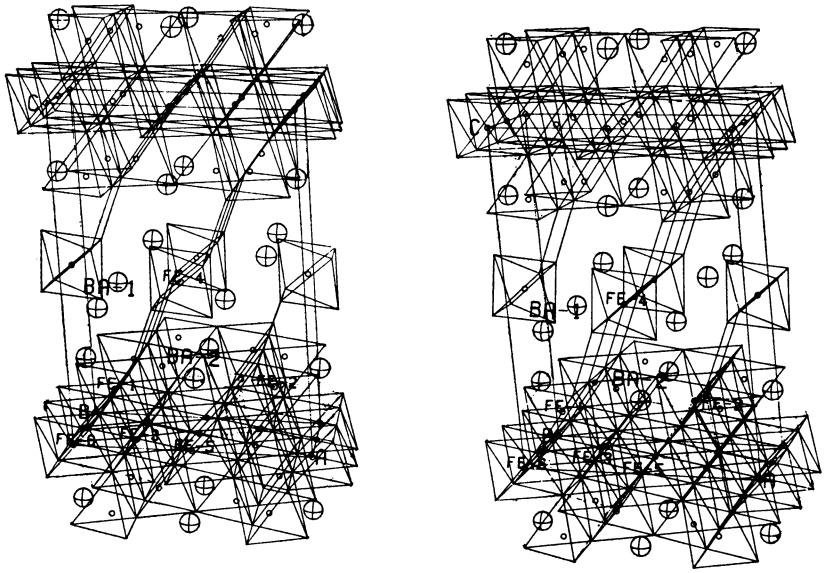

Fig. 3. Stereoscopic drawing of the crystal structure of $Ba_4Fe_9O_{20}H_6$.

$Fe(OH)_6^{3-}$ cluster between these layers. Interatomic distances are summarized in Table 4.

Ba(1) and Ba(2) are surrounded respectively by nine and ten oxygen atoms at distances ranging from 2.61 to 3.02 Å. It is noticeable that each Ba is close to one oxygen atom, with a separation of less than 2.70 Å. Similar situations occur in $BaFe_2O_4$ obtained by firing,[3] in $Ba_2[Al_2(OH)_{10}]$[12], and $Ba_3[Al_2(OH)_{12}]$,[13] both grown from aqueous solutions, and in $Ba(OH)_2 \cdot 8H_2O$.[14] On the other hand, in hexagonal barium ferrites,[15] such a close contact of Ba to O is not found, but their structures are close-packed build-ups of O and Ba: for example, in $Ba_2Zn_2Fe_{12}O_{22}$ (ofen referred to as Y ferrite), Ba is surrounded by twelve oxygens at distances between 2.95 and 3.26 Å.[16]

The coordination octahedron around Fe(4) consists of four equivalent oxygen atoms [O(3)] in equatorial positions and two O(6) atoms in axial positions. This octahedron is much more regular than the other Fe octahedra and does not share any vertices, edges, or faces with the adjacent polyhedra. These findings strongly suggest that all vertices of the octahedron around Fe(4) are occupied by OH groups. The equatorial oxygen O(3) in the cluster is close to O(2) in the triple layer, at a distance of 2.872 Å, and forms a weak hydrogen bond, while the axial oxygen O(6) does not participate in any hydrogen bond. This hydrogen-bonding scheme is quite consistent with the IR spectrum described above. Each of the four equivalent hydrogen bonds is shown in the stereoscopic drawings of Fig. 3, together with the $Fe(OH)_6^{3-}$ clusters, Ba^{2+} ions, and triple layers of condensed ferrite anions.

One would expect the Fe–O distances to provide a powerful assistance for establishing the position of Fe

TABLE 4. INTERATOMIC DISTANCES (l/Å)

(a) Ba–O distances		
Ba(1)–O(5)	2.611(25)	*once*
–O(3^{iv})	2.741(18)	*twice*
–O(3)	2.906(14)	*twice*
–O(6^{iv})	3.011(3)	*twice*
–O(3^{v})	3.065(15)	*twice*
Ba(2)–O(6^{vi})	2.687(31)	*once*
–O(4)	2.753(23)	*once*
–O(1^{i})	2.756(16)	*twice*
–O(2)	2.989(14)	*twice*
–O(2^{i})	3.005(13)	*twice*
–O(5^{i})	3.015(3)	*twice*
(b) Fe–O distances		
Fe(1) octahedron		
Fe(1)–O(2)	1.941(14)	*twice*
–O(5)	1.942(23)	*once*
–O(4)	2.134(26)	*once*
–O(1)	2.183(16)	*twice*
Fe(2) tetrahedron		
Fe(2)–O(2^{i})	1.868(13)	*twice*
–(5^{ii})O	1.868(19)	*once*
–O(7)	1.921(30)	*once*
Fe(3) octahedron		
Fe(3)–O(1)	2.004(16)	*twice*
–O(4)	2.011(16)	*twice*
–O(7^{iii})	2.041(17)	*twice*
Fe(4) octahedron		
Fe(4)–O(6)	2.007(30)	*twice*
–O(3)	2.022(14)	*4 times*
Fe(5) octahedron		
Fe(5)–O(4)	2.120(23)	*twice*
–O(1^{i})	2.134(14)	*4 times*
Fe(6) octahedron		
Fe(6)–O(1)	1.996(12)	*4 times*
–O(7^{iii})	2.006(25)	*twice*
(c) Me–Me distances (l<4.0 Å)		
Ba(1)–Fe(1)	3.548(7)	*once*
–Fe(4^{v})	3.615(2)	*twice*
–Fe(4)	3.749(3)	*once*
Ba(2)–Fe(5)	3.174(4)	*once*
–Fe(2)	3.407(5)	*once*
–Fe(1)	3.458(5)	*once*
–Fe(2^{ix})	3.461(5)	*twice*
–Fe(1^{i})	3.514(3)	*twice*
Fe(1)–Fe(3)	3.064(5)	*twice*
–Fe(6)	3.085(5)	*once*
–Ba(2)	3.458(5)	*once*
Fe(2^{v})	3.458(3)	*twice*
Fe(2^{vii})	3.490(6)	*once*
–Ba(2^{ix})	3.514(5)	*twice*
–Ba(1)	3.548(7)	*once*
Fe(2)–Ba(2)	3.407(5)	*once*
–Fe(6^{ii})	3.454(6)	*once*
–Fe(3^{iii})	3.457(5)	*twice*
–Fe(1^{i})	3.458(3)	*twice*
–Ba(2^{i})	3.461(5)	*twice*
–Fe(1^{ii})	3.490(6)	*once*
Fe(3)–Fe(5)	2.970(1)	*twice*
–Fe(6)	2.970(1)	*twice*
–Fe(3^{x})	2.993(2)	*twice*
–Fe(1)	3.064(5)	*twice*
–Fe(2^{iii})	3.457(5)	*twice*
Fe(4)–Ba(1^{i})	3.615(2)	*4 times*
–Ba(1)	3.749(3)	*twice*
Fe(5)–Fe(3)	2.790(1)	*4 times*
–Fe(6^{i})	2.993(2)	*twice*
–Ba(2)	3.174(3)	*twice*
Fe(6)–Fe(3)	2.970(1)	*4 times*
–Fe(5^{ix})	2.993(2)	*twice*
–Fe(1)	3.085(5)	*twice*
–Fe(2^{iii})	3.454(6)	*twice*

(d) A hydrogen bond

O(3)–O(2) 2.873(27)

symmetry code			
none	x,	y,	z,
i	$\frac{1}{2}+x$,	$-\frac{1}{2}+y$,	z,
ii	$1+x$,	y,	z,
iii	$1-x$,	$-y$,	$-z$,
iv	$\frac{1}{2}-x$,	$\frac{1}{2}-y$,	$1-z$,
v	$-\frac{1}{2}+x$,	$-\frac{1}{2}+y$,	z,
vi	$1-x$,	$-y$,	$1-z$,
vii	$-1+x$,	y,	z,
viii	$-x$,	$-y$,	$1-z$,
ix	$-\frac{1}{2}+x$,	$\frac{1}{2}+y$,	z,
x	x,	$-y$,	z,

with oxidation number two. All Fe–O distances in the tetrahedron (mean 1.88 Å) and octahedra (mean 2.01 Å) other than those concerning Fe(1) and Fe(5) are nearly equal to those of Fe with oxidation number three, as reported in the literature.[17] On the other hand, distances of Fe–O concerning Fe(5) are significantly larger (2.12—2.13 Å), in fair agreement with typical values for Fe with oxidation number two. Hence, the position of Fe with oxidation number two could be confirmed to be in the middle slice of the triple layer. As a consequence, the formula should be written $Ba_4[Fe^{III}(OH)_6][Fe^{II}Fe_7^{III}O_{14}]$. This finding suggests that Ba^{2+} ions, $[Fe(OH)_6]^{3-}$ ions, and some condensed ferrite anions with sheet-like structures exist generally in the hydrothermal medium.

The Fe–O distances around Fe(1) vary from 1.941 to 2.183 Å. In this octahedron, O–O distances of the shared edges in the basal plane are shorter than those of the unshared edges in the top plane which faces toward the outside of the triple layer. The Fe(1) is displaced toward the outside of the triple layer, so that Fe(1) is closer to the three oxygens of the shared vertices (1.942 and twice 1.941 Å) than to those of the shared edges (2.134 and twice 2.183 Å). Such a variety of Fe–O distances was also found in α-Fe_2O_3[18] and in two modifications of $BaFe_4O_7$.[5] In the former case, where two FeO_6 octahedra are stacked by sharing their faces, the distortion was explained in terms of a

large electronic interaction between two Fe across the shared plane. The repulsion between Fe^{3+} and Ba^{2+} might cause an additional distortion in the structure of both modifications of $BaFe_4O_7$. In the present case, however, the distances of Fe(1)–O can not be understood only by such local interactions. This suggests that the three Fe(1)–O bonds concerning the oxygen atoms shared by FeO_4 tetrahedra are more covalent than the other three.

Polymerization of ferrite anions has been discussed by many workers.[19-21] On the basis of the structure of $Ba_4[Fe(OH)_6][Fe_8O_{14}]$ determined just above, we suppose three stages of condensation of ferrite anions, such as the following: (1) The free hydroxo-complex anion, $[Fe(OH)_6]^{3-}$, found in solution is enclosed into nuclei of the lattice together with Ba^{2+} cations. (2) The condensation of the hydroxo-complex anions proceeds with accompanying dehydration, and the FeO_6 octahedra necessarily share their vertices or edges with each other. (3) During such a condensation process, a part of the FeO_6 octahedra are allowed to convert into FeO_4 tetrahedra, as evidenced by the Fe(2) tetrahedra kept back in the crystal lattice. If all FeO_6 octahedra transform to FeO_4 tetrahedra sharing their vertices, then the resulting framework of condensed ferrites would become tetrahedral chains or a two- or three-dimensional network analogous to silicates, aluminosilicates, and aluminates. Such a situation is encountered in barium monoferrite, $BaFe_2O_4$, obtained by firing. We have recently found another example of a three-dimensional framework of FeO_4 tetrahedra in $Ba_8Fe_{13}O_{30}H_6$[5] synthesized by a hydrothermal reaction.

Magnetic Properties. The easy axis of magnetization was examined by a combined use of an optical microscope and a hand permanent magnet. Batches of samples were classified into two groups because of their quite remarkably different magnetizations; the easy magnetization axes of one batch of samples lay on the basal plane of the hexagonal plates, while those of the other batch were directed toward the outside of the plane. The single crystal used for this X-ray study was obtained from the former; its easy magnetization axis pointed in the a-direction. The latter batch of crystals emerged less frequently. These distinct groups of samples showed somewhat different Mössbauer spectra; these are compared in Fig. 4. Such a difference can not be explained in terms of a preferred orientation of the sample grains. It is therefore probable that two modifications would occur, owing to only slight differences in either the contents or the locations of Fe atoms with oxidation number two. Although the Mössbauer spectra are quite complicated, a tentative assignment was made for three Fe species by assuming that the oxidation numbers of all Fe are three and that their isomer shifts are in the range of $0.0<\delta<0.7$ mm s^{-1} (referred to Fe foil). Considering the numbers of equivalent positions and the coordination number of oxygens, we assigned the three Fe species to Fe(2), Fe(1), and Fe(3) in the increasing order of δ. The Mössbauer parameters thus obtained are given in Table 5.

The magnetic measurement was made only for crystals

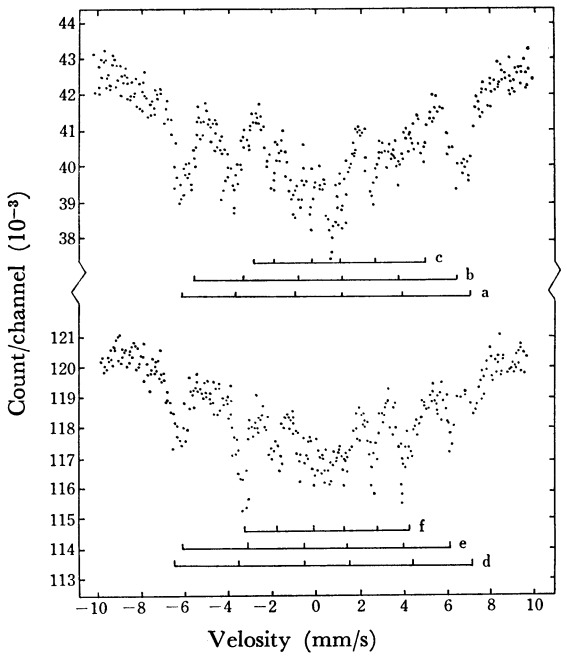

Fig. 4. Mössbauer spectra of $Ba_4Fe_9O_{20}H_6$.
Above: crystals with easy magnetization axes directed toward out of the (001) plane. Below: crystals with easy magnetization axes lying the (001) plane.

Table 5. Mössbauer parameters of $Ba_4Fe_9O_{20}H_6$

Spectra (in Fig. 4)	Isomer shift[a] ε/mm s^{-1}	Quadrupole splitting δ/mm s^{-1}	Inner field H_{int}/kG[b]
a	0.37	−0.16	413
b	0.31	−0.11	380
c	0.09	−0.33	346
d	0.21	0.06	425
e	0.23	0.11	383
f	0.30	0.10	313

a) with respect to the centroid of the spectrum of iron foil at 293 K. b) $1G=10^{-4}$ T.

with easy axes parallel to the (001) plane. The variation of magnetization against field strength was measured from 900 to 12000 G at room temperature. The value stayed constant at 13.80 ± 0.05 emu g^{-1} above 2000 G and saturation was considered to be reached. Figure 5 shows the temperature dependence of magnetization from 77 to 573 K measured at 4000 G, together with the Néel point, $T_N=515$ K. This plot is far from a Langevin curve, indicating complicated mechanisms of magnetic interaction. An extrapolation of this curve gives a magnetic moment of about 10 μ_B per formula corresponding to just two Fe^{3+} ions. If the magnetic moments are simply ordered parallel and antiparallel below T_N, then a space group of P2/m with the same cell dimensions or doubling of the unit sell in volume would be required for the magnetic unit cell.

Twining. Twinning of this crystal would be expected to occur in various ways, owing to the pseudo-hexagonal symmetry possessed by the triple layer of the condensed ferrite anion in the structure (the axial

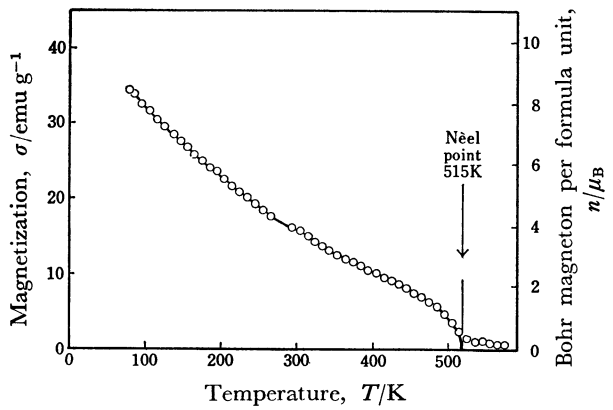

Fig. 5. Variation of magnetization at 4000 G with temperature.

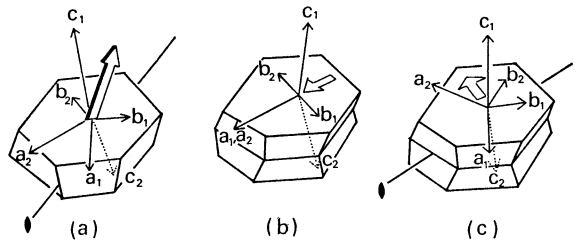

Fig. 6. Three twin laws of $Ba_4Fe_9O_{20}H_6$.
(a) [110] axial twinning. (b) Twin and composition plane (001). (c) [130] axial twinning. Directions of easy magnetization axes are shown by open arrows. Twin axes are shown by diad axes in (a) and (c).

ratio of a/b is 1.714). In fact three kinds of twin laws were confirmed by X-ray techniques, and the direction of the easy magnetization axis for each twinned specimen was determined by use of a permanent magnet. Relative orientations of individual crystals, which were determined by Weissenberg and precession photographs, are shown in Fig. 6 together with the direction of easy magnetization. The first kind is the [110] axial twinning; here the easy direction is perpendicular to the twin axis, but it leans at an angle of about 30° from the normal of the (001) plane (Fig. 6a). The second is not axial, and the (001) plane corresponds to the twin and composition plane (Fig. 6b). In this case, the a-axes of both individuals are coincident and the easy magnetization axis is parallel to this direction. The third twinning is [130] axial twinning, in which the easy magnetization axis is perpendicular to the twin axis and lies on the (001) plane (Fig. 6c). It is plausible that twinning repeats during the crystal growth according to these laws. Many sorts of polysynthetic twins were found very often under an optical microscope. In addition, the latter two kinds of twins appeared as a mixture in a batch, while the first appeared in a different batch. The direction of easy magnetization can not be explained solely on the basis of a vector sum of individual contributions. This finding also suggests the occurrence of two or more modifications in this compound.

The authors thank Dr. Masayasu Tokonami of this Institute for his assistance in the X-ray intensity data collection. The authors also thank Dr. Hideko Kiriyama of this Institute for her helpful criticisms of the manuscript.

References

1) Y. Goto and T. Takada, *J. Am. Ceram. Soc.*, **43**, 150 (1960); S. Mori, *ibid.*, **49**, 600 (1966).
2) J. Smit and H. P. J. Wijn, "Ferrites," International ed., Tokyo Electrical Enginnering Press, Tokyo (1965), p. 117.
3) H. Mitsuda, S. Mori, and C. Okazaki, *Acta Crystallogr.*, **B27**, 1263 (1971).
4) K. Kitahama and R. Kiriyama, *Acta Crystallogr.*, **A28**, S62 (1972).
5) S. Okamoto, S. I. Okamoto, and T. Ito, *Acta Crystallogr.*, **B29**, 832 (1973).
6) S. Okamoto, H. Sekizawa, and S. I. Okamoto, *J. Phys. Chem. Solids*, **36**, 591 (1975).
7) R. Kiriyama, T. Tsai, and K. Kitahama, *Ferrites*: Proc. Intern. Conf. 1970, Japan, p. 171, Univ. Tokyo Press (1971).
8) G. C. Kennedy, *Am. J. Sci.*, **248**, 540 (1950); **255**, 724 (1957).
9) "International Tables for X-Ray Crystallography," Vol. IV, Kynoch Press, Birmingham (1974), pp. 71—98 and 148—150.
10) T. Sakurai, Ed., "UNICS Program System," Crystallographic Society of Japan (1967).
11) C. K. Johnson, ORTEP. Oak Ridge National Laboratory Report ORNL-3794 (1965).
12) A. H. Moinuddin Ahmed and L. S. Dent Glasser, *Acta Crystallogr.*, **B26**, 867 (1970).
13) A. H. Moinuddin Ahmed and L. S. Dent Glasser, *Acta Crystallogr.*, **B25**, 2169 (1969).
14) H. Manohar and S. Ramaseshan, *Z. Kristallogr., Kristallgeom., Kristallphys., Kristallchem.*, **119**, 357 (1964).
15) P. B. Braun, *Philips Research Repts.*, **12**, 491 (1957).
16) W. D. Townes and J. H. Fang, *Z. Kristallogr., Kristallgeom., Kristallphys,. Kristallchem.*, **131**, 196 (1970).
17) R. D. Shannon and C. T. Prewitt, *Acta Crystallogr.*, **B25**, 925 (1969).
18) R. L. Blake, R. E. Hessevick, T. Zoltai, and L. W. Finger, *Am. Mineral.*, **51**, 123 (1966).
19) K. Inouye, *Kagaku to Kogyo*, **27**, 571 (1974).
20) H. Schuger, C. Walling, R. B. Jones, and H. B. Gray, *J. Am. Chem. Soc.*, **1967**, 3712.
21) K. M. Towe and W. F. Bradley, *J. Colloid Interface Sci.*, **24**, 384 (1967).